

# BRITTLE FRACTURE STRENGTH OF NOTCHED ROUND BAR UNDER AXIAL LOAD

M. Aoki and A. Kiuchi

*Structural Engineering Laboratory, Kobe Steel Ltd., Amagasaki, Hyogo, Japan*

## ABSTRACT

The brittle fracture strengths of circumferentially notched round bar (CNRB) and surface notched round bar (SNRB), which are subjected to axial load, have been investigated over a range of temperature by using two kinds of steel bars. The curve showing the relationship between nominal net section stress at fracture,  $\sigma_{nF}$ , and temperature,  $T$ , macroscopically consists of the three regions both for CNRB and SNRB. Final fracture surface is cleavage in Region I and II, and ductile in Region III. While  $\sigma_{nF}$  diminishes with decreasing  $T$  in Region I, it is nearly constant in Region II. The effect of diameter of bar,  $D$ , and relative notch depth on  $\sigma_{nF}$  in Region I can be evaluated by applying the linear fracture mechanics technology. Meanwhile,  $\sigma_{nF}$  in Region II does not depend on  $D$  very much, but on relative notch depth. The effect of relative notch depth on  $\sigma_{nF}$  in Region II both for CNRB and SNRB is approximately evaluated from the experimental formulae on the basis of the stress level at general yielding.

## KEY WORDS

Round bar; brittle fracture; circumferential crack; surface crack; axial load; steel bar.

## INTRODUCTION

When steel bars such as bolt, wire and tie-rod are used as structural members at low temperature, it is needed to assess the brittle fracture strengths of them.

In this report, the engineering procedure of evaluating the brittle fracture strengths of circumferentially notched round bar (CNRB) and surface notched round bar (SNRB) under axial loading was established over a range of temperature.

## EXPERIMENTS

### Material

The materials tested are steel bars for tie-rod (hereafter referred to as SMn443) and for bolts and shafts (SCM440).

Table 1 Chemical Compositions and Mechanical Properties

Steel	Dia mm	Chemical compositions %									Mechanical properties*			
		C	Si	Mn	P	S	Cu	Ni	Cr	Mo	$\sigma_y$ kgf/mm <sup>2</sup>	$\sigma_a$ kgf/mm <sup>2</sup>	EL %	R.A. %
SMn443	50	0.39	0.25	1.57	0.023	0.004	0.01	0.02	0.17	-	53.8	77.2	20.0	62
SCM440	50	0.40	0.23	0.71	0.018	0.009	0.01	0.02	1.03	0.20	96.0**	106.8	15.6	69

\* Gage length: 50mm, Diameter of specimen: 8.0mm \*\* 0.2% proof stress

The chemical compositions and mechanical properties are presented in Table 1. The fracture appearance transition temperature in Charpy-V test at the central portion of bar is about 30°C for SMn443 and -55°C for SCM440.

Test Specimen and Test Procedures

Firstly, the fracture toughness was evaluated by COD bend test (NB test) as shown in Fig. 1. NB test specimens of 6mm thickness were employed to examine the distribution of fracture toughness along the radial direction in the steel bars. Secondly, the effect of diameter of bar, D, and notch depth, on the brittle fracture strength of CNRB and SNRB under axial loading was studied on specimens as shown in Fig. 2. In addition, the effect of notch acuity on the brittle fracture strength of CNRB was studied on specimens with and without fatigue crack at the tip of the machined notch (radius of notch tip : 0.1mm).

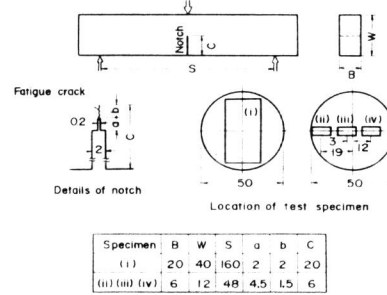


Fig. 1 COD bend test specimen

The fatigue precracking of each specimen was carried out under pulsating (0 to tension), where the stress intensity factor at maximum load is within the range of 60 to 80 kgf/mm<sup>3/2</sup>. The precracked specimen was cooled at the specified temperature for about 10min., and loaded to fracture. The opening displacement near the edge of notch,  $V_g$ , was measured by means of a clip gage and recorded continuously against load. For NB tests,  $V_g$  at fracture was converted into the value at the crack tip,  $\delta_c$ , by using the formulae developed by Wells (1971). When a maximum load plateau is obtained, the opening displacement at the first attainment of maximum load plateau was taken as a critical value. Meanwhile, in case of CNRB and SNRB,  $V_g$  at fracture was not converted into  $\delta_c$ .

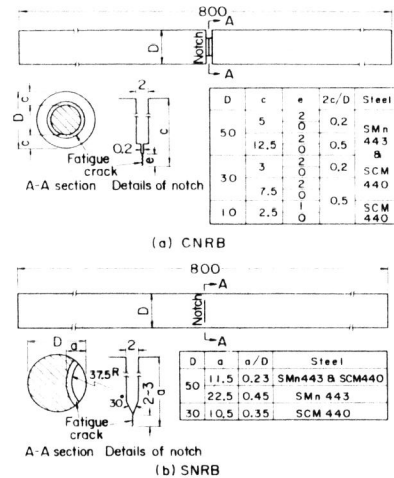


Fig. 2 Circumferentially notched and surface notched round bar

TEST RESULTS AND DISCUSSION

COD Bend Tests

$\delta_c$  of SMn443 and SCM440 is shown in Fig. 3 as a function of temperature. Open points denote the

averaged  $\delta_c$  of three specimens of 6mm thickness. It is found that  $\delta_c$  increases with increasing distance from the central axis of round bar, r, and that  $\delta_c$  of 20mm thick specimen is smaller than  $\delta_c$  of 6mm thick one on account of so-called thickness effects.

When the radial distribution of fracture toughness is represented in terms of  $\delta_c/(\delta_c)_{r=12}$  ( $(\delta_c)_{r=12}$  denotes  $\delta_c$  at  $r = 12\text{mm}$ ), it was reduced to similar linear relationship of r for SMn443 and SCM440. Moreover, when the relationship is rearranged by using  $\delta_c$  at  $r=r_0$ ,  $(\delta_c)_{r=r_0}$ , in place of  $(\delta_c)_{r=12}$ , it is expressed by eq. (1).

$$\frac{\delta_c}{(\delta_c)_{r=r_0}} = \frac{r + 15.8}{r_0 + 15.8} \quad (1)$$

Since the fracture toughness,  $K_{Ic}$ , is proportional to the square root of  $\delta_c$ , eq. (1) can be written as follows:

$$\frac{K_{Ic}}{(K_{Ic})_{r=r_0}} = \sqrt{\frac{r + 15.8}{r_0 + 15.8}} \quad (2)$$

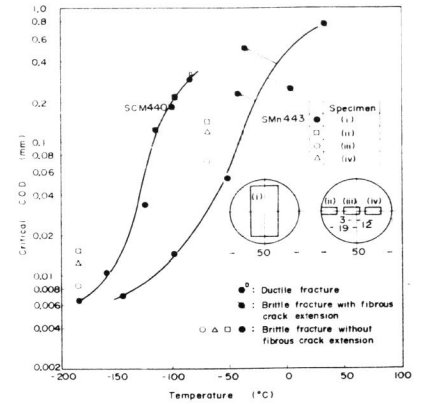
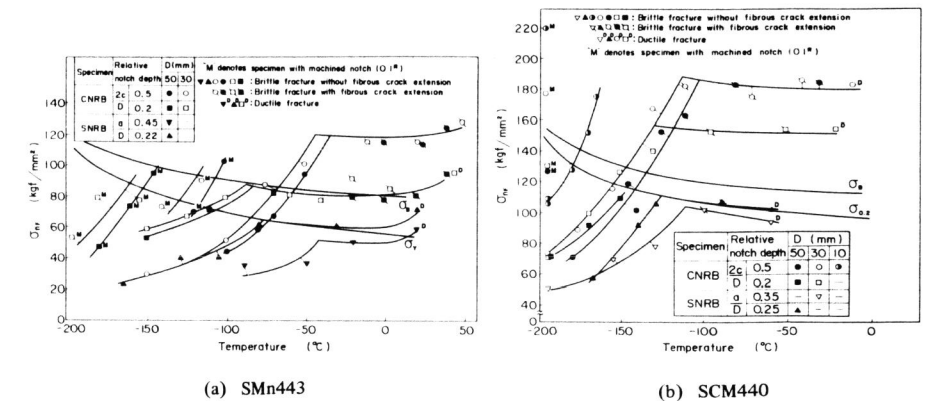


Fig. 3 Temperature dependence of critical COD

Tensile Tests of Circumferentially Notched Round Bar

The nominal net section stress at fracture,  $\sigma_{NF}$ , for SMn443 and SCM440 is shown as a function of temperature, T, in Fig. 4. Test results of SNRB to be mentioned later are also shown in these figures. The curve showing the relationship between  $\sigma_{NF}$  and T,  $\sigma_{NF}$ -T curve, macroscopically consists of the three regions both for CNRB and SNRB.

- Region I :  $\sigma_{NF}$  decreases with decreasing T and fracture surface is cleavage.
- Region II :  $\sigma_{NF}$  is nearly constant irrespectively of T, and final fracture surface is cleavage.
- Region III : ductile fracture region.



(a) SMn443

(b) SCM440

Fig. 4 Relationship between fracture stress and temperature

Next, the effects of D, 2c/D (c : notch depth) and notch acuity on the brittle fracture strength are investigated. The linear fracture mechanics is considered to be applicable in Region I, but not in Region II.

**Estimation of fracture stress in Region I.** The stress intensity factor, K, of CNRB under axial load is expressed by eq. (3) (Bueckner, 1965).

$$K = \frac{\pi}{4} \sqrt{D} \sigma_n \left\{ 1.72 \frac{d}{D} - 1.27 \left( \frac{d}{D} \right)^2 \right\} \quad (3)$$

where  $\sigma_n$  : nominal applied stress at notched section, d : diameter of notched section (= D-2c).

Meanwhile,  $K_C$  was estimated by substituting  $\delta_c$  value obtained from NB tests of 20mm thickness into  $\delta_c$  in eq. (4).

$$K_C = \sqrt{m \cdot \delta_c \cdot E \cdot \sigma_Y} \quad (4)$$

where E : Young's modulus,  $\sigma_Y$  : yield stress at the temperature concerned, m : plastic constraint factor (in case of converting  $V_B$  at fracture into  $\delta_c$  by using the formulae after Wells,  $m \approx 1.7$  (for example, Steel Sectional Meeting of the Japan Welding Society, 1979)).

NB test specimens of 20mm thickness were prepared so that the middle part of crack front of the specimen may coincide with the central axis of round bar. Therefore,  $\delta_c$  from the NB test specimens is considered to be dominated by the toughness around the middle part of crack front, which has comparatively lower toughness and higher triaxiality (Ikeda and colleagues, 1978).  $K_C$  at the position of a given distance, r, can be obtained by substituting  $K_C$  in the central position of bar calculated from eq. (4) into  $(K_C)_{r=0}$  of eq. (2). By setting K expressed by eq. (3) equal to  $K_C$  at the crack front of CNRB,  $\sigma_{nF}$  can be estimated for a given value of D and 2c/D. Estimated  $\sigma_{nF}$ ,  $(\sigma_{nF})_{Est.}$ , is compared with experimental one,  $(\sigma_{nF})_{Exp.}$ , in Fig. 5 (a).  $(\sigma_{nF})_{Est.}$  is higher than or equal to  $(\sigma_{nF})_{Exp.}$ . Therefore, this estimation results in nonconservative one. This is presumably because the constraint to plastic flow for CNRB is higher than that for NB test specimen.

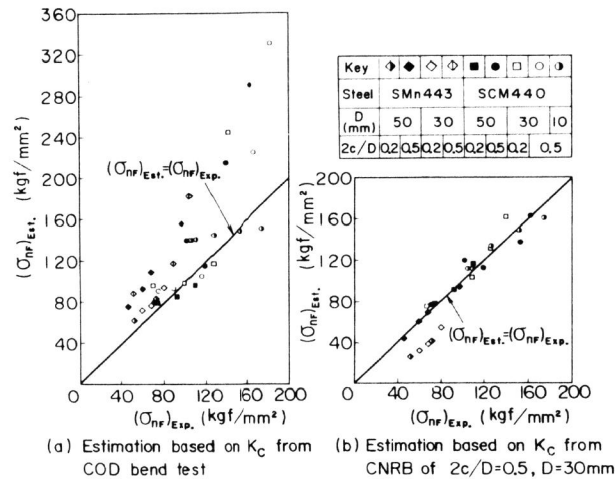


Fig. 5 Comparison of estimated fracture stress with experimental one for CNRB (Region I)

Then,  $(\sigma_{nF})_{Est.}$  of CNRB with various D and 2c/D was calculated on the basis of  $K_C$  of CNRB for D = 30mm and 2c/D = 0.5.  $(K_C)_{CNRB}$ . In this calculation,  $K_C$  at the crack front of CNRB with various D and 2c/D was obtained by substituting  $(K_C)_{CNRB}$  into eq. (2) in which  $r_0$  was taken as 7.5mm. The comparison of  $(\sigma_{nF})_{Est.}$  with  $(\sigma_{nF})_{Exp.}$  is made in Fig. 5 (b).  $(\sigma_{nF})_{Est.}$  obtained on the basis of  $(K_C)_{CNRB}$  agrees well with  $(\sigma_{nF})_{Exp.}$ , except the case of 2c/D = 0.2 for SMn443 (◆ ◇). This case, however, results in the conservative estimation.

Fig. 4 also shows that  $\sigma_{nF}$ -T curve of CNRB with fatigue crack in Region I locates in the higher temperature range by 40 to 60°C than that for CNRB with machined notch both for SMn443 and SCM440. It is concluded that the effect of notch acuity on  $\sigma_{nF}$  in Region I is remarkable.

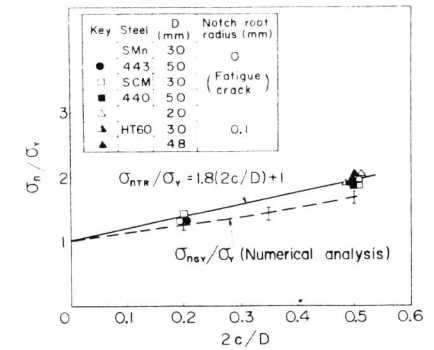


Fig. 6 Notch yield ratio at transition temperature,  $\sigma_{nTR}/\sigma_Y$ , as a function of relative notch depth (CNRB)

**Estimation of fracture stress in Region II.** It can be seen from Fig. 4 that  $\sigma_{nF}$  of CNRB is higher than that for SNRB in Region II, because the constraint to plastic flow around the notch is enhanced by the effect of the geometry of CNRB.  $\sigma_{nF}$  of CNRB at the transition point from Region I to Region II, which appears as the discontinuous point of  $\sigma_{nF}$ -T curve, is denoted by  $\sigma_{nTR}$ . Ratio of  $\sigma_{nTR}$  to  $\sigma_Y$ ,  $\sigma_{nTR}/\sigma_Y$ , as a function of 2c/D for SMn443 and SCM440 is shown in Fig. 6. In this figure, the results of the tests conducted in the cooperative research committee of the Japan Welding Society (1975) are also shown. In the research,  $\sigma_{nF}$ -T curve was obtained on CNRB (2c/D = 0.5, machined notch) of three kinds of diameter which were taken from the plate of mild steel and several high strength steels. It was found from the test results that  $\sigma_{nTR}/\sigma_Y$  was within the range of 1.9 through 2.1 irrespectively of  $\sigma_Y$  and D.  $\sigma_{nTR}/\sigma_Y$  for 60 kgf/mm<sup>2</sup> high strength steel is shown as a typical example in Fig. 6. In addition, the nominal net section stress at general yielding,  $\sigma_{nGY}$ , of CNRB was analyzed with the aid of computer program for wide application, MARC (1981), in which 8-node isoparametric element was used. The ratio of  $\sigma_{nGY}$  to  $\sigma_Y$ ,  $\sigma_{nGY}/\sigma_Y$ , as a function of 2c/D is also shown in Fig. 6.  $\sigma_{nTR}/\sigma_Y$  seems to be determined by 2c/D only and increases linearly with an increase of 2c/D. This tendency is the same as that obtained from the numerical analysis. Furthermore,  $\sigma_{nTR}/\sigma_Y$  is a little higher than  $\sigma_{nGY}/\sigma_Y$ . This implies that the transition from Region I to Region II occurs right after general yielding. The relationship between  $\sigma_{nTR}/\sigma_Y$  and 2c/D was approximated with the following experimental formula:

$$\sigma_{nTR}/\sigma_Y = 1.8 (2c/D) + 1 \quad (5)$$

$\sigma_{nF}/\sigma_Y$  in Region II increases slightly with increasing T, since  $\sigma_Y$  decreases as T increases. Therefore,  $\sigma_{nF}$  in Region II can be estimated conservatively by multiplying the value of  $\sigma_{nTR}/\sigma_Y$  by  $\sigma_Y$  at the temperature concerned. Fig. 6 also shows that  $\sigma_{nTR}/\sigma_Y$  for fatigue crack is almost equal to that for machined notch. Therefore, the machined notch with 0.1mm tip radius is considered to be equivalent to the fatigue crack from a viewpoint of the brittle fracture strength in Region II.

**Tensile Tests of Surface Notched Round Bar**

**Estimation of fracture stress in Region I.** Firstly, K value of SNRB under axial load was analyzed with the aid of MARC, in which 20-node isoparametric element was used. It was found from the observation of the fracture surface that fracture of SNRB under axial load initiated from the vicinity of the deepest point of surface crack front, which had lower toughness and higher constraint to plastic flow in comparison with the crack front near the specimen surface. Therefore, K value at the deepest point of surface crack front was evaluated in this study. K value normalized by gross tensile stress,  $\sigma_g$ , and notch depth, a, is shown in Fig. 7 as a function of relative

notch depth,  $a/D$ , and radius of curvature of surface crack front,  $R$ . Clark (1977) analyzed experimentally  $K$  value for SNRB of 12.8mm dia. with a straight crack front. As shown in Fig. 7, the results of the present analysis agree well with those of the experimental one after Clark. For comparison,  $K$  value for surface notched plate (SNP) with  $R = 0.75t$  ( $t$ : thickness of plate) and  $R = \infty$ , which was analyzed by Newman & Raju (1981) and Gross et al. (1964), respectively, is also shown in Fig. 7. Although there is no wide difference of  $K$  value between SNRB and SNP for  $R = \infty$ , it seems that the difference becomes large with increasing  $a/D$  for finite  $R$ . Meanwhile, in the range of small  $a/D$  or  $a/t$ ,  $K$  value for SNRB and SNP agrees approximately each other. This implies that  $K$  value for small  $a/D$  or  $a/t$  shows little change with the configuration of notched section. Therefore, it is considered that  $K$  for SNRB also tends to about 1.12 in the same manner as  $K$  for SNP when  $a/D$  approaches to zero.  $K$  value for SNRB as a function of  $a/D$  and  $R$  is expressed with a polynomial approximation of eq. (7), assuming that  $K$  equals to 1.12 at  $a/D = 0$ .

$$K = M\sigma_g \sqrt{\pi a} \quad (6)$$

$$M = 1.12 + \{0.30/D - 1.85/R\} a - \{6.63/D^2 - 10.25/(R \cdot D)\} a^2 + \{23.13/D^3 - 18.75/(R \cdot D^2)\} a^3 \quad (7)$$

where  $R \geq 0.5D$  for  $a/D \leq 0.4$   
 $R \geq 0.75D$  for  $0.4 < a/D \leq 0.6$

$K$  value for SNRB mentioned above was analyzed under uniform tensile stress, namely it is a solution for pin-end loading. Meanwhile, the fracture tests of SNRB were conducted under the condition of fixed grip loading. When SNRB is subjected to uniform tensile stress, bending stress occurs additionally with tensile stress at the notched section. Therefore,  $K$  value under uniform tensile stress is larger than that under fixed grip loading. However, the latter approaches to the former as the distance between grip ends becomes long. It was confirmed by additional numerical analysis that  $K$  value under uniform tensile stress is approximately applicable for that under fixed grip loading in the present fracture tests.

Secondly,  $K_C$  at the deepest crack front of SNRB was obtained by substituting  $K_C$  in the central portion of bar calculated from eq. (4) into  $(K_C)_{r=R_0}$  of eq. (2).  $\sigma_{nF}$  may be estimated by setting  $K$  of eq. (6) equal to

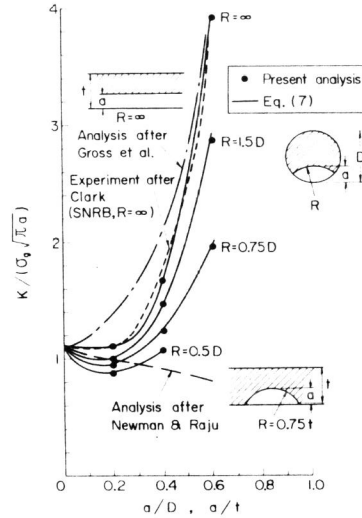


Fig. 7 Stress intensity factor for SNRB under uniform tensile stress

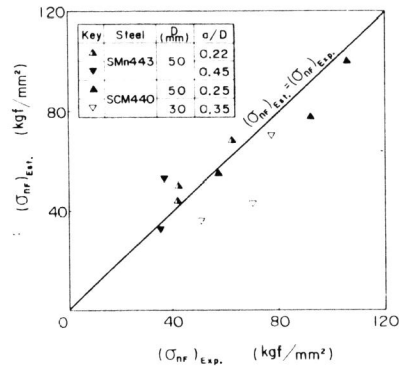


Fig. 8 Comparison of estimated fracture stress with experimental one for SNRB (Region I)

the  $K_C$ . The comparison between estimated  $\sigma_{nF}$  and experimental  $\sigma_{nF}$  for SNRB is made as shown in Fig. 8. Both values agree approximately. Therefore, the brittle fracture strength in Region I for SNRB under axial load can be evaluated on the basis of  $K_C$  obtained from NB test unlike the case of CNRB, because SNRB has lower constraint to plastic flow than CNRB.

**Estimation of fracture stress in Region II.** Region II can be said to be the region where the brittle fracture initiates after general yielding. In case of the tensile tests on CNRB, the transition from Region I to Region II occurred right after general yielding as mentioned before. Next, the effects of  $D$  and  $a/D$  on  $\sigma_{nGY}$  for SNRB are discussed below. The relationship between  $\sigma_{nGY}$  and relative notch depth for single edge notched plate (SENP) has been evaluated from the slip line theory and the numerical analysis using finite element method, but that for SNRB has not yet. Authors and colleagues (1982) solved the equation of yielding condition for SNRB with  $R = \infty$ , which is subjected to uniform tensile stress. As a result, eq. (8) was derived.

$$(\sigma_{nGY}/\sigma_Y^*)^2 + h (\sigma_{nGY}/\sigma_Y^*) = 1 \quad (8)$$

$$\text{where } h = \frac{(D^2/4 - b^2)^{3/2}}{2(D^2/4 - \bar{y}^2)^{3/2} - 3\bar{y} \left\{ 0.39D^2 - \left( \bar{y} \sqrt{D^2/4 - \bar{y}^2} + \frac{D^2}{4} \arcsin \frac{2\bar{y}}{D} \right) \right\}} \quad (9)$$

$\sigma_Y^*$ : yield stress enhanced by the intensified constraint caused by existence of notch,  
 $b$ : distance from the central axis of round bar to the crack front ( $= D/2 - a$ ),  
 $\bar{y}$ : distance from the central axis of round bar to the center of gravity at notched section

$$\left( = \frac{2(D^2/4 - b^2)^{3/2}}{3 \left\{ (\pi - \arccos \frac{2b}{D}) \frac{D^2}{4} + b \sqrt{D^2/4 - b^2} \right\}} \right) \quad (10)$$

Since  $h$  in eq. (9) is a function of  $a/D$  only,  $\sigma_{nGY}/\sigma_Y^*$  is also given as a function of  $a/D$  only from eq. (8). In Fig. 9, the relationship between  $\sigma_{nGY}/\sigma_Y$  and  $a/D$  calculated from eq. (8) is shown by broken line marked with ratio of  $\sigma_Y^*$  to uniaxial yield stress,  $\sigma_Y$ , ( $\sigma_Y^*/\sigma_Y = \alpha$ ). In the figure, the experimental data  $\sigma_{nF}/\sigma_Y$  in Region II are also shown. However, round bar with a semicircular crack front was regarded as that with a straight one so that bending stress at the notched section may be nearly equal each other. Furthermore, additional SNRB specimens with  $R = \infty$  of the piano wire (SWRS77B) were tested at 0°C, which fractured in a brittle manner. In Fig. 9, these test results are also shown. The relationship between  $\sigma_{nF}/\sigma_Y$  and  $a/D$  in Region II seems to be expressed with a curve given by eq. (8) of  $\alpha = 1.25$  irrespectively of  $D$  and kinds of steels. However,  $\alpha$  should tend to 1 when  $a/D$  approaches to zero. Therefore, the upper limit of  $\sigma_{nF}/\sigma_Y$  was assumed to be 1. For reference, the relationship between  $\sigma_{nGY}/\sigma_Y$  and relative notch depth for SENP, which was analyzed from the slip line theory by Ewing et al. (1974), is also shown by the dotted line in Fig. 9. It nearly corresponds to a curve given by eq. (8) of  $\alpha = 1.1$ .

CONCLUSIONS

The brittle fracture strengths for circumferentially notched round bar (CNRB) and surface notched round bar (SNRB), which are subjected to axial load, have been investigated over a range of temperature. The following conclusions were drawn:

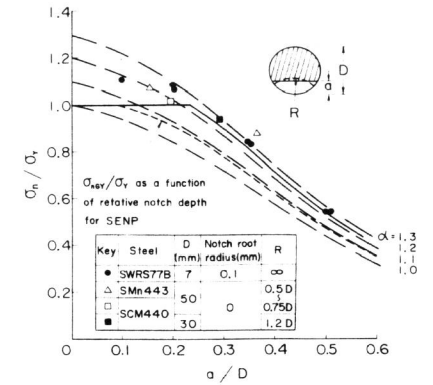


Fig. 9 Notch yield ratio in Region II as a function of relative notch depth (SNRB)

- (1) The curve showing the relationship between nominal net section stress at fracture,  $\sigma_{nF}$ , and temperature macroscopically consists of three regions both for CNRB and SNRB  
 Region I :  $\sigma_{nF}$  decreases with decreasing temperature and fracture surface is cleavage.  
 Region II :  $\sigma_{nF}$  is nearly constant irrespectively of temperature and final fracture surface is cleavage.  
 Region III : ductile fracture region.  
 Region II can be said to be the region where the brittle fracture initiates after general yielding.  $\sigma_{nF}$  for CNRB is higher than that for SNRB in Region II and III, because CNRB has higher constraint to plastic flow than SNRB.
- (2) The effects of diameter of bar, D, and relative notch depth on  $\sigma_{nF}$  in Region I can be evaluated by applying the linear fracture mechanics technology.
- (3)  $\sigma_{nF}$  in Region II does not depend on D very much, but on relative notch depth. As the relative notch depth increases,  $\sigma_{nF}$  increases in case of CNRB but decreases in case of SNRB. The effect of relative notch depth on  $\sigma_{nF}$  may be approximately evaluated from the experimental formulae derived on the basis of stress level at general yielding.

#### REFERENCES

- Bueckner, H.F. (1965). ASTM STP381, 82.
- Clark, Jr. W.G. (1977). ASTM STP 631, 128.
- Ewing, D.J.F. and C.E. Richards (1974). Journal of the Mechanics and Physics of Solids, Vol. 22, 27 - 36.
- Gross, B., J.E. Strawley and W.F. Brown, Jr. (1964). NASA Technical Note D-2395.
- Ikeda, K. and colleagues (1978). The Third International Symposium of the Japan Welding Society, 155 - 160.
- Kiuchi, A. and colleagues (1982). Journal of the Iron and Steel Institute of Japan, Vol. 68, No. 13, 156 - 164.
- MARC Analysis Research Corporation (1981). MARC General Purpose Finite Element Program, Vol. A - E, Rev. J. 2.
- Newman, Jr. J.C. and I.S. Raju (1981). Engineering Fracture Mechanics, Vol. 15, No. 1 - 2, 185 - 192.
- Steel Sectional Meeting of the Japan Welding Society (1979). Report of JI Committee.
- Steel Sectional Meeting of the Japan Welding Society (1975). Report of TM Committee.
- Wells, A.A. (1971). 3rd Canadian Congress on Appl. Mech., Calgary.